

# CHAPTER-IV

## MAGNETIC PROPERTIES

## CHAPTER-IV

### MAGNETIC PROPERTIES

#### SECTION: A : MAGNETISATION STUDIES :

##### 4.1 INTRODUCTION :

The data collected from hysteresis loops exhibited by a magnetic material provide information regarding saturation magnetisation, remanent magnetisation, coercive force. Magnetisation is considered to be fundamental property of oxide spinel ferrites, which belong to ferrimagnets. The magnetic materials can be divided into two groups :

- 1) SOFT (Magnetically) : Which are easy to magnetise and demagnetise
- 2) HARD (Magnetically) : Which are difficult to magnetise and demagnetise.

In case of ferrites, the ferrite with low coercive force are termed as soft ferrites and find their use in high frequency inductance, core of transformers motors and generators. The ferrites with high coercive force are called as hard ferrites and are used in electric motors, loudspeakers, telephone and as permanent magnets.

##### 4.2 THEORETICAL ASPECT :

Neel<sup>1</sup> in 1949 has shown that the coercive force is related with saturation magnetisation, internal stresses and porosity of material. The squareness of hysteresis loop decides its

suitability in magnetic memory and switching devices, Maxwell<sup>2</sup> suggested experimental method for measurement of magnetic properties of ferrites.

When a magnetic substance acquires magnetisation  $M$  in presence of applied field  $H$ , then ,

$M = \chi H$  where  $\chi$  is susceptibility of material. If  $\chi$  is small and negative the substance is diamagnetic. If  $\chi$  is small and positive, the substance is paramagnetic.

If  $\chi$  is large and positive, substance is self saturating and consist domains in demagnetised state and is called as ferromagnetic substance.

If  $\chi$  is small and positive at all temperatures and lattice of magnetic ion breaks into A and B sites with stronger tendency towards antiparallelism, the substance is called as antiferromagnetic.

If  $\chi$  is large and positive, lattice of magnetic ions breaks into A and B sublattices with their magnetic moments antiparallel and of different magnitude, the substance is called as ferrimagnetic. The above classification of magnetic materials is based on magnetic order and spontaneous magnetisation. The possible spin arrangements in magnetic materials is shown in Fig. 4.1

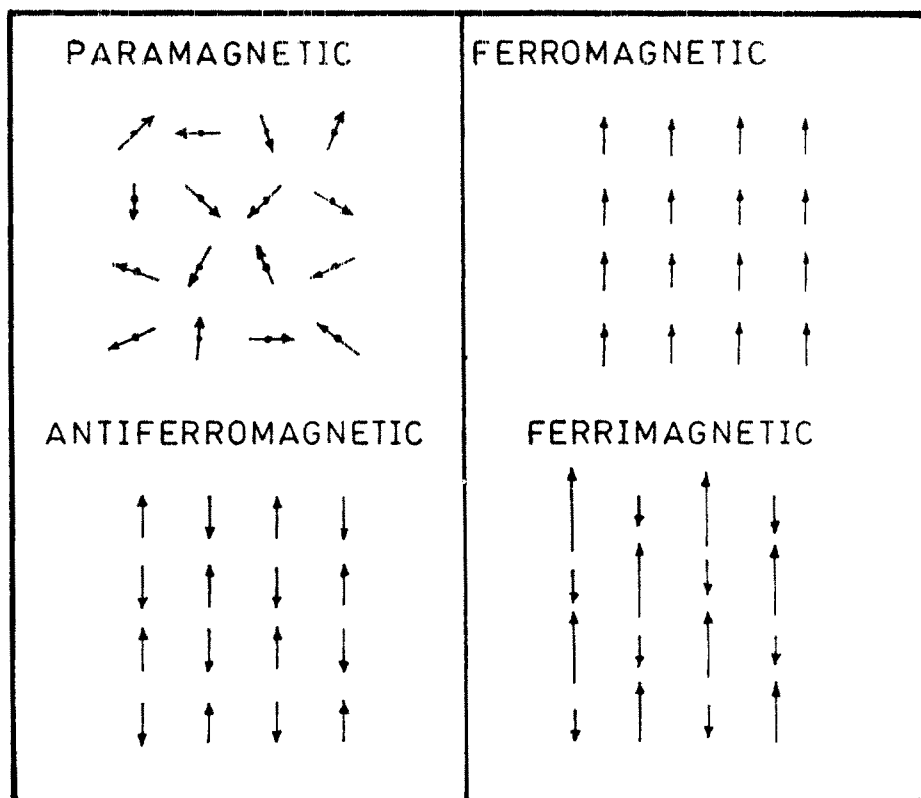


Fig. 4-1

Weiss<sup>3</sup> explained spontaneous magnetisation on the basis of existence of molecular field. Heisenberg<sup>4</sup> gave quantum mechanical treatment to explain alignment of moments in terms of exchange interaction between the uncompensated spins of electrons in partially filled 3d shell. Neel<sup>5</sup> showed that spontaneous magnetisation in antiferromagnetic and ferrimagnetic substances can arise as a result of negative exchange interactions. In ferrites the spontaneous magnetisation arise as a result of antiparallel arrangements of magnetic moments resulting in their partial compensation. The magnetisation is mainly due to magnetic moments arising from spin magnetic moment.

Gorter<sup>6,7,8,9</sup> Pauthéut<sup>10,11</sup> Smit and Wijn<sup>12</sup> and Others<sup>13-22</sup> studied and obtained saturation moments of several ferrites  $\text{Me}_x\text{Zn}_{1-x}\text{Fe}_2\text{O}_4$  where Me is divalent metal ion such as Cu, Ni, Co, Cd, Mg, Mn etc. Fallot and Marconi<sup>23</sup> showed that Neel's theory is not suitable for temperature dependence near Curie temperature in paramagnetic region. Guillaud and Creveaux<sup>24</sup> measured magnetisation as a function of temperature for several mixed ferrites over large range of temperature and composition in ferrimagnetic region. The decrease in magnetic moment is attributed to formation of paramagnetic clusters and non linear spin cluster<sup>25,26,27</sup> and site presence of cation<sup>28</sup>. Sawant S.R. and Patil R.N.<sup>21</sup> have reported that non collinear magnetic structure is responsible for magnetic behaviour of Cu substituted  $\text{Ni}_x\text{Zn}_{1-x}\text{Fe}_2\text{O}_4$  as suggested Yafet and Kittel<sup>29</sup>.

#### 4.3 MAGNETIC PROPERTIES :

##### Magnetocrystalline anisotropy :

Magnetic properties of a substance depend on the direction in which they are measured. The term "Anisotropy" is often used in his connection. Magnetocrystalline anisotropy is intrinsic to the material and is of importance for explaining permeability and coercive force. The magnetocrystalline or anisotropy energy is the difference between the energy required to magnetise the sample to saturation along the hard direction and that required along an easy direction. For ferrite with cubic crystal structure, Anisotropy energy.

$$W_k = K_1 \left( \alpha_1^2 \alpha_2^2 + \alpha_2^2 \alpha_3^2 + \alpha_3^2 \alpha_1^2 \right) + K_2 \alpha_1^2 \alpha_2^2 \alpha_3^2 + \dots$$

where  $K_1$  and  $K_2$  are anisotropy constants, characteristics of a particular material and  $\alpha_1, \alpha_2, \alpha_3$ , the direction cosines of magnetisation vector with respect to cubic axis.

$$E_k = K_1 \sin^2 \theta$$

where  $K_1$  - Anisotropy constant

$\theta$  - Angle between L and S.

Zener<sup>30</sup> studied the influence of the temperature variation of saturation magnetisation on that of anisotropy constant. He showed that anisotropy constant "K" decreases much faster with increasing "T" than does saturation magnetisation  $M_s$ .

#### 4.4 DOMAIN THEORY :

Weiss<sup>3</sup> introduced a novel idea : Magnetic domain, to explain spontaneous magnetisation, which was further confirmed experimentally. A ferromagnetic material is considered to be consisting of small regions (domains) each of which is at all times completely magnetised in a particular direction. Magnetic domains are separated by domain walls. Magnetisation of material under an applied field take place by motion of domain walls and its rotation. By dividing ferromagnetic crystal into several domains, its magnetic energy is reduced to minimum.

Weiss<sup>3</sup> postulated presence of internal molecular field for explaining spontaneous magnetisation. The state of zero magnetisation in ferromagnetic crystal led to the prediction of randomly oriented domains. Barkhausen<sup>31</sup> gave experimental evidence of existence of domains.

Weiss<sup>3</sup> explained spontaneous magnetisation on the basis of hypothetical molecular field . Heisenberg<sup>32</sup> gave quantum mechanical approach in terms of exchange interaction between uncompensated electron spins in partially filled 3d shells. The exchange interactions, which occur in crystal lattice give rise to exchange energy. Exchange energy,

$$W_{ex} = 2J_e S^2 \sum_{i \neq j} \cos \theta_{ij}$$

where S - Total spin momentum per atom

$\theta_{ij}$  - Angle between spin momentum vector of atom i & j

The positive exchange interaction give rise to ferromagnetism  
 -ve exchange interaction give rise to antiferromagnetism spontaneous  
 magnetisation arise through negative exchange interactions tending  
 to make neighbouring magnetic moments antiparallels. This suggest  
 origin of spontaneous magnetisation in ferrites.

#### 4.5 DOMAIN WALL ENERGY :

Eloch<sup>33</sup> in 1932 showed that the entire change in spin  
 direction between domains magnetised in different directions does  
 not occur in one sudden jump a cross single plane, but takes  
 place in a gradual way extending over many atomic planes. This  
 wall of finite width contain spins whose orientation gradually  
 change from the direction in one domain to that in other. Thus  
 atomic spin within wall do not remain parallel to an easy direction  
 and lead to an isotropy energy. The thickness of domain wall  
 is determined by condition of minimum total energy.

Domain wall energy

$$E_w = 4/(AK)^{1/2}$$

where A - Exchange energy constant.

K - Anisotropy constant.

#### 4.6 IRREVERSIBILITY :

The irrerversibility in wall motion is due to nonmagnetic  
 inclusions, defects, dislocations. Kersten<sup>34</sup> proposed model of  
 wall motion in homogeneous materials containing inclusions. He



showed change in energy of domain wall results in the variation of wall area. Neel calculated critical field  $H_C$  required for irreversible domain wall movement and coercivity with the help of dispersed field theory. Goodenough concluded that granular inclusion, lamellar precipitates, grains boundaries, crystal faces are most likely centres of reverse domain formation.

#### 4.7 MAGNETIC HYSTERESIS :

Magnetic hysteresis of a ferromagnetic material refer to the lag in change in magnetic induction behind the change in intensity of external magnetising field due to the dependence of magnetic induction on its past history. Magnetic hysteresis is a result of irreversible changes that take place in magnetisation and demagnetisation of magnetic material.

When a ferromagnetic substance is subjected to an external field, its magnetisation increases with increase in magnetic field, reaches a saturation value at a certain critical field. On reducing the external magnetic field, demagnetisation is not effected completely. Thus the magnetisation appears to lag behind the applied field. Such a behaviour exhibited by ferromagnetic substance in course of a complete cycle of magnetisation and demagnetisation and is called as "Magnetic hysteresis." Fig.4.2

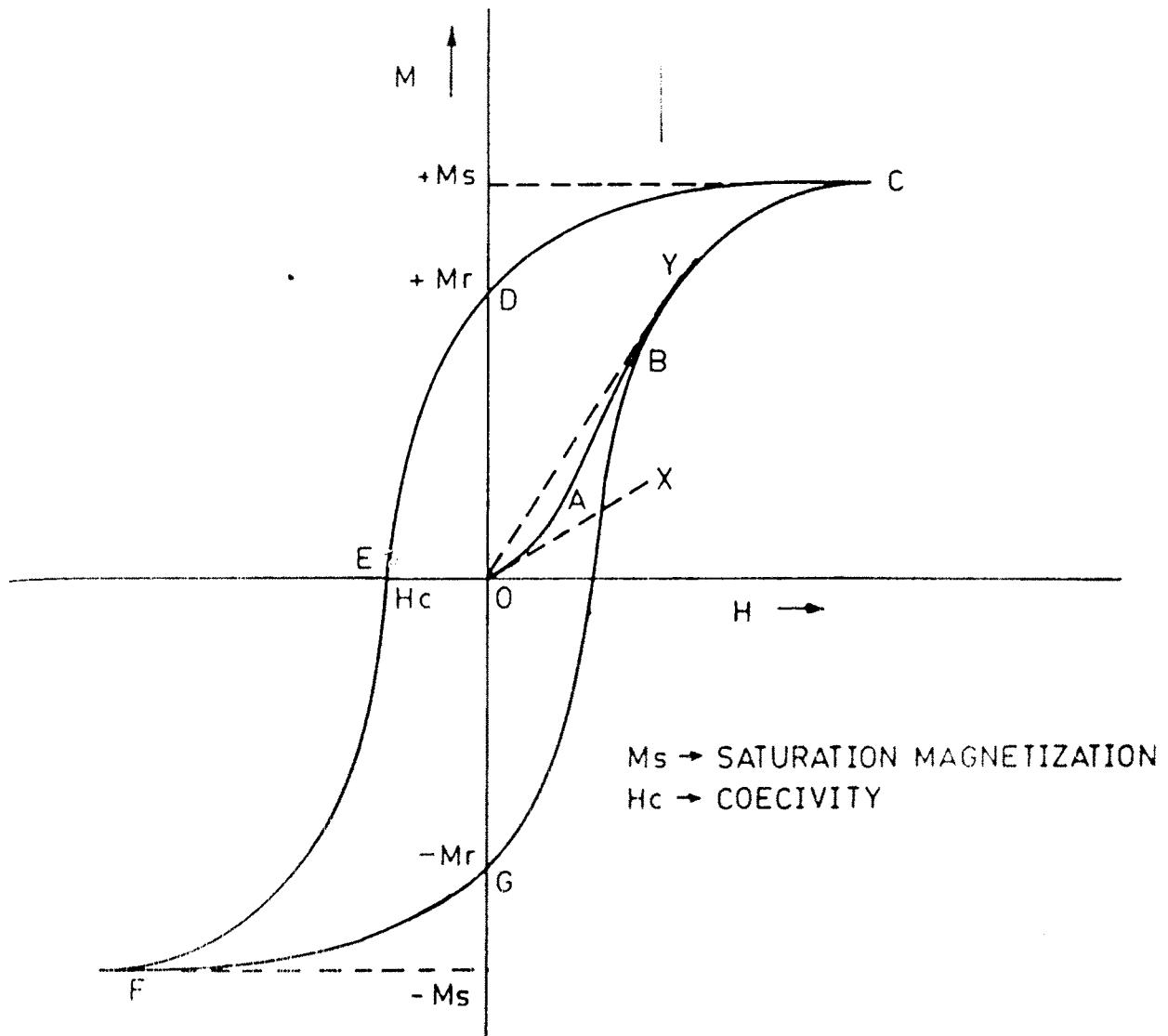


FIG.42: MAGNETIZATION CURVE (OABC) AND  
HYSTERESIS LOOP (CDEFGC)

#### 4.8 COERCIVITY :

Coercive force is a function of grain size of a polycrystalline material. Coercive force increases with decreasing particle size, reaches to a maximum and then tends to zero. The variation of coercive force with particle size is depicted in Fig. Fig.4.3

##### Multidomain (M-D) :

Magnetisation of a specimen containing multidomain particles changes by domain wall motion and follows the relation,

$$H_c = a + b/D$$

where a and b = constant

D= particle diameter.

##### Single Domain (S-D) :

When particle diameter reduces below critical diameter  $D_s$ , reaches to single domain particle size,  $H_c$  will be maximum. The decrease in coercivity below critical diameter is attributed to thermal effect in accordance with the relation,

$$H_c = g - h/D^{3/2}$$

where g and h are constants

When particle diameter is below  $D_p$ , coercive force  $H_c$  is zero and attributed to thermal effects. In this stage thermal effects

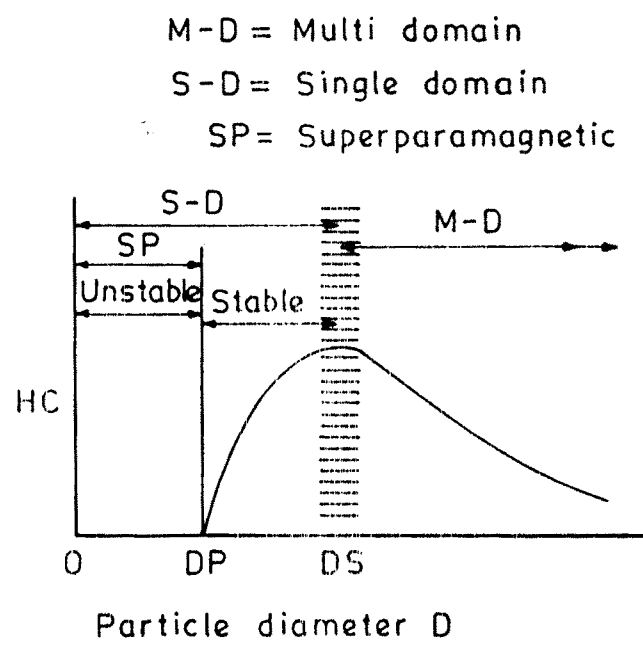


Fig.4.3 : VARIATION OF COERCIVITY WITH  
PARTICAL DIAMETER

are strong enough to demagnetise already saturated assembly of particles and the particle size is referred to as super paramagnetic(SP) Coercive force is influenced by shape anisotropy.

#### 4.9 LOSSES IN MAGNETIC MATERIALS :

When a magnetic material is subjected to an alternating magnetic field, material absorbs certain amount of energy, and dissipate it in the form of heat.

Consider an alternating magnetic field represented by,

$$H = H_0 \exp i \omega t$$

Then induction B can be written as,

$$B = B_0 \exp i (\omega t + \delta)$$

Permeability,

$$\mu = B/H = (B_0 / H_0) (\cos \delta + i \sin \delta)$$

$$\mu = \mu' + i \mu''$$

Where  $\mu'$  - component of magnetic flux which is in phase with applied field.

$\mu''$  - component of magnetic flux which is  $90^\circ$  out of phase with applied field.

The power factor or loss factor,

$$\tan \delta = \mu'' / \mu'$$

and

$$Q = 1 / \tan \delta = \mu' / \mu''$$

The magnetic permeability spectrum include the variation of  $\mu'$  and  $\mu''$  with frequency. The significant losses in magnetic material are :

1. Hysteresis loss
2. Eddy current loss
3. Spin-resonance loss
4. Relaxation loss
5. Wall resonance loss

#### 4.9(a) HYSTERESIS LOSS :

To change magnetisation from  $M$  to  $M + dM$  in an applied field  $H$ , the energy required is given by,

$$dE = H \cdot dM$$

Total energy absorbed in a complete hysteresis cycle is,

$$W = \oint H \cdot dM = \text{Area of hysteresis loop.}$$

Low coercive force ( $H_c$ ) or high permeability ( $\mu$ ) or high susceptibility ( $\chi$ ) results in smaller area under the loop and hence low hysteresis loss. Hysteresis loss appears as heat causing a temperature rise of the order of  $10^{-4}$  °C per gram per cycle in case of metals.

#### 4.9(b) EDDY CURRENT LOSS :

When alternating magnetic field is applied to a magnetic core materials, an electric current is induced in material, which

causes a power loss. This is called as eddy current loss. The power loss per second is proportional to  $f^2/\rho$  where  $f$  is frequency of applied a.c. field and  $\rho$  the electrical resistivity of the material of core, The power loss is given by,

$$P = A (f^2/\rho)$$

The constant of proportionality  $A$  depends on the shape of core.

#### 4.9(c) SPIN RESONANCE LOSS :

The precessional frequency  $\omega$  of an electron spin vector in presence of internal anisotropy field  $H_k$  is given by,

$$2\pi f_r = \omega = \gamma H_k$$

where  $\gamma$  - gyromagnetic ratio

$H_k$  - internal anisotropy field.

$H_i$  - External field magnetic field ( $H_k \perp H_i$ )

If  $H_i$  is alternating field with frequency equal to  $f_r$ , resonance sets in and energy is absorbed from applied field and dissipated in the material. For a material with negative anisotropy constant rotational process are important and resonant frequency is inversely proportional to  $(\mu - 1)$

#### 4.9(d) RELAXATION LOSS :

These losses are exhibited at frequencies much lower than resonant frequency and are attributed to several relaxation process. Major relaxation loss in ferrite is attributed to electron exchange between  $Fe^{2+}$  and  $Fe^{3+}$  ions for minimum energy, which

result in change in direction of magnetisation. The relaxation loss is frequency dependent.

#### 4.9(e) WALL RESONANCE LOSS :

In some ferrites, domain wall resonance loss is found to occur at low frequency. If domain wall is disturbed from its equilibrium position, it develops a restoring force, which try to bring the wall back to its equilibrium position. The domain wall behave as stretched elastic membrane having natural frequency of oscillation. When frequency of applied field matches natural frequency of domain wall, resonance occurs reading to maximum absorption of energy.

#### 4.10 EXPERIMENTAL :

The measurements of  $M_s$ ,  $M_r$  and  $H_c$  were carried out using high field loop tracer. The loop tracer consist of an electromagnet capable of working on 50 Hz mains supply the sinusoidal magnetic field of about 3600 oersted is produced in the air gap of 9 mm in the instrument and a special balancing coil is used to measure the saturation magnetisation of the sample in air gap. The signal from balancing coil after integration the is proportional to magnetization of /specimen and is fed to the Y plates of oscilloscope after suitable amplification. A signal proportional to magnetic field is fed to the X plates of oscilloscope. The oscilloscope displays magnetization against magnetising



field i.e. hysteresis loop for the sample. The vertical deflection can be calibrated in terms of magnetic moment in e.m.u. and horizontal in gauss per division. The measurement magnetic parameters are accurate within five percent.

Thus in short the assembly consist of :

- i) C- core unit to feed the sample and to amplify signal,
- ii) Control unit to supply the power
- iii) Display unit-CRO to observe the hysteresis loop and to carry out quantitative measurement with the help of digital multimeter.(Plate -1)

Measurement procedure :

To start with high voltage cable is connected from control unit to C-core unit. Balancing coil is mounted on 12 pin connector associated with C -core unit and introduced in an air gap in an instrument. The vertical and horizontal output of C core unit are fed to vertical and horizontal inputs of control unit respectively. The vertical output is connected to vertical input of the oscilloscope and horizontal output to EXT horizontal keeping vertical gain control at low positive, current is increased upto 200 mA using control unit so as to get an ellipse on screen. To convert ellipse into straight line, the vertical phase control is adjusted. The straightline is rotated to make phase difference zero by adjusting "coarse"

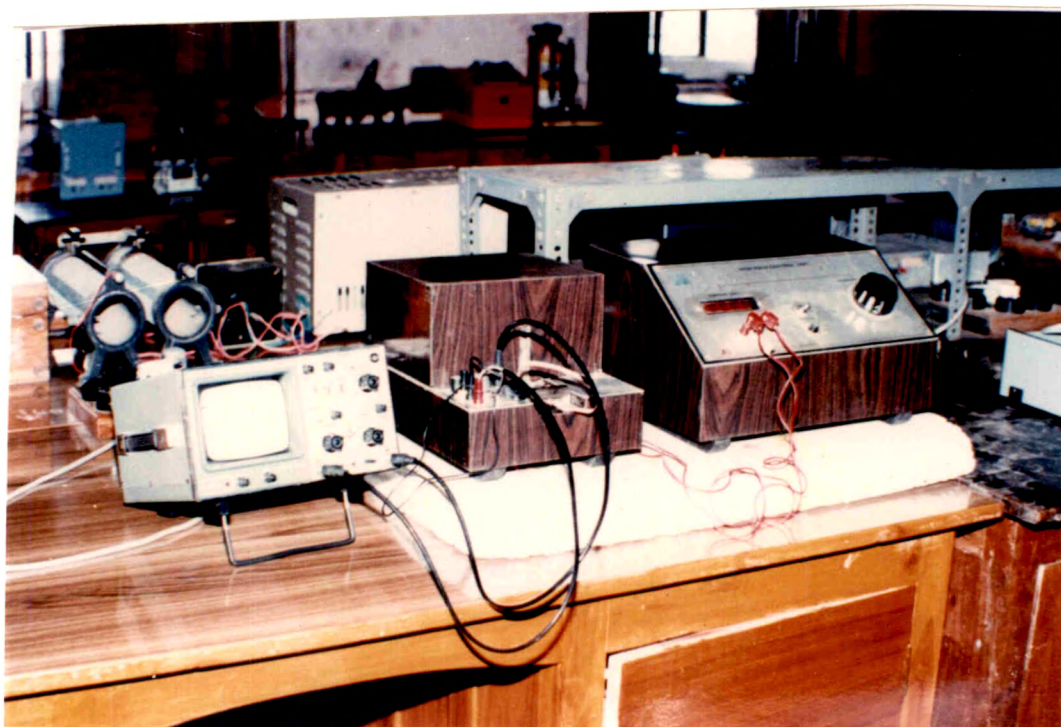


PLATE - II



amplitude potentiometer. Then balancing coil is taken out of C core gap.

The measurement were carried out directly on C.R.O. screen. standard Nickel sample having saturation magnetisation of 53.34 e.m.u./gm was used for calibration of C.R.O screen. When current through the coil of magnet was 200 mA. The current was gradually increased and hysteresis loop was obtained on C.R.O. screen. Thus the C.R.O. displays magnetization versus magnetizing field i.e. hysteresis loop for sample. Without disturbing experimental assembly, hysteresis loops were obtained for all the samples and corresponding measurements were made.

#### 4.11 RESULTS AND DISCUSSION :

The saturation magnetisation values  $M_s$  magnetic moment  $n_B$  were obtained and are presented in Table 4.1. The experimental values of magnetic moment were obtained by using formula,

$$n_B = \frac{\text{Molecular weight} \times M_s}{5585 \times ds}$$

where  $ds$  = density of sample

$$M_s = \text{saturation magnetisation in e.m.u.per cm}^3$$

saturation magnetisation  $M_s$  was calculated by using formula,

$$M_s = (1 - P) \sigma_s ds$$

where  $P$  = porosity

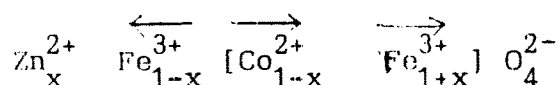
$$\sigma_s = \text{saturation magnetisation e.m.u. per gram.}$$

TABLE 4.1  
VALUES OF MAGNETISATION, MAGNETIC MOMENT

Composition	Dopant	$n_B$ Bohr Magneton	$M_s$ emu/gram	$4 \pi M_s$
$Co_{0.5}Zn_{0.5}Fe_2O_4$	No	2.58	212.5	2670.8
	0.05 At. wt. % Al	2.34	211.8	2662.0
	0.05 mol. Wt. % $Gd_2O_3$	2.72	249.1	3130.0
$Co_{0.7}Zn_{0.3}Fe_2O_4$	No	4.39	399.58	5021.0
	0.05 At. Wt. % Al	4.02	378.47	4756.0
	0.05 mol. Wt. % $Gd_2O_3$	4.63	433.1	5442.0
$CoFe_2O_4$	No	3.47	292.4	3674
	0.05 At. wt. % Al	3.18	288.3	2623.0
	0.05 mol. Wt. % $Gd_2O_3$	3.63	399.38	5006.0

NOTE : Sample  $ZnFe_2O_4$  and  $Co_{0.3}Zn_{0.7}Fe_2O_4$  either undoped or doped  
don't show magnetisation at room temperature

It is seen that saturation magnetisation varies as expected attaining maximum value when the zinc content in  $\text{Co}_x\text{Zn}_{1-x}\text{Fe}_2\text{O}_4$  system is 0.5. The cation distribution is given by Smith and Wijn<sup>12</sup>. Taking into consideration zinc occupies tetrahedral site (A-site) is as follows.



The arrows indicate direction of magnetic moment. From above formula one should expect for zinc ferrite saturation magnetisation  $n_B = 10$  per molecule. This situation will never occur due to mutual negative interactions of the octahedral spins. The magnetic behaviour is due to presence of A-B magnetic behaviour is due to presence of A-B and B-B interactions and their relative strength. For lower concentration of Zinc A-B interaction is dominant and as zinc concentration is increased, A-B interaction goes on decreasing. At a certain concentration of zinc A-B and B-B interaction will become equal and above that concentration B-B interaction becomes dominant due to which spins will align antiparallel of B site and hence the material will get transformed into paramagnetic substance. Similar behaviour is observed, in present system and the samples  $\text{ZnFe}_2\text{O}_4$  and  $\text{Co}_{0.3}\text{Zn}_{0.7}\text{Fe}_2\text{O}_4$  show a paramagnetic behaviour at room temperature. Maximum value of magnetisation is observed for  $\text{Co}_{0.5}\text{Zn}_{0.5}\text{Fe}_2\text{O}_4$ . This variation may be due to the difference in method of preparation, heat treatment etc.

For Aluminium doped samples, magnetic moment and corresponding magnetisation reduces, whereas for Gadolinium doped samples it increases in comparison with undoped samples. This may be explained as follows. Our I.R. studies shows that trivalent impurity ion  $\text{Al}^{3+}$  and  $\text{Gd}^{3+}$  ion reduce  $\text{Fe}^{3+}$  ions on octahedral site. The electronic configuration of these three are  $[\text{Ne or } 1s^2 2s^2 2p^6]$ ,  $[\text{Xe } 4f^7]$  and  $[\text{Ar } 3d^5]$  respectively.

It is seen that Aluminium ion is diamagnetic, whereas  $\text{Gd}^{3+}$  and  $\text{Fe}^{3+}$  ions are paramagnetic. Comparing  $\text{Fe}^{3+}$  and  $\text{Gd}^{3+}$  ion it is seen that there are two extra spins associated with  $\text{Gd}^{3+}$  ion. As such one can expect magnetic moment and hence magnetisation  $\text{Gd}_2\text{O}_3$  doped sample to increase, and Al doped sample decrease in comparison with undoped version.

## SECTION : B : SUSCEPTIBILITY :

## 4.12 INTRODUCTION :

For magnetic materials in fields that are not extensively strong,

$$\text{Magnetization } M = \chi H$$

where  $\chi$  is magnetic susceptibility of the substance

Susceptibility is a unique property of magnetic materials and is the ratio of intensity of magnetisation  $M$  and applied field  $H$ . For diamagnetic substance susceptibility is negative or zero and is independent of temperature. For paramagnetic substance susceptibility is positive and depends on temperature. The temperature dependence of susceptibility in case of paramagnetic material is given by,

$$\chi = C/T \quad \text{Curie law}$$

where  $C$  is Curie constant. The value of  $C$  from quantum statistics was predicted by Maxwell as,

$$C = \mu_{\text{eff}}^2 M_s / 3k$$

where  $\mu_{\text{eff}}$  - effective value of magnetic moment

$M_s$  - Saturation magnetization.

For paramagnetic material the effective magnetic moment

$$\mu_{\text{eff}} = g \sqrt{J(J + 1)} \mu_B$$

where notations have usual meanings.

On the basis of spin ordering, magnetic materials are subdivided into ferromagnetic, antiferromagnetic and ferrimagnetic substances.

Ferromagnetic and ferrimagnetic materials exhibit spontaneous magnetisation below Curie temperature. Antiferromagnetic materials have no resultant spontaneous magnetisation, because of compensation of equal and opposite magnetic moments.

The variation of susceptibility in ferromagnetic material is temperature dependent and is given by,

$$\chi = C/(T - T_c)$$

This expression is based on Weiss molecular field in ferro and ferrimagnetic substance.

For antiferromagnetic substance,

$$\chi = C/(T + T_c)$$

positive sign is due to antiparallel coupling of magnetic spins. Ferrites are ferrimagnetic substances below Curie temperature. Above Curie temperature magnetic transition from ferrimagnetic to paramagnetic occurs. Several methods to measure Curie temperature  $T_c$  exist in literature<sup>35,36</sup>. Still susceptibility and resistivity studies also give satisfactory values of transition or Curie temperature. Also a.c. magnetic susceptibility studies<sup>37</sup> gives an account of magnetic behaviour of material, ferrimagnetic to paramagnetic transition, single domain to super paramagnetic transition, R.G.Kulkarni et al<sup>38</sup> have reported a.c. susceptibility studies on Co-Ca ferrites, Cu-Cd ferrites and spinel systems



$\text{Ge}_x\text{Cu}_{1-x}\text{Fe}_2\text{O}_4$ . R.S. Chaugule et al<sup>39,40</sup> have reported a.c. magnetic susceptibility and hysteresis studies on  $\text{La}_{1-x}\text{Y}_x\text{Mn}_2\text{Si}_{12}$  intermetallic compound and found multidomain (MD), single domain (SD) and super paramagnetic (SP) states present in the material. S.R. Sawant et al<sup>41</sup> have carried out a.c. susceptibility and magnetisation studies on Cu-Zn ferrites. C. Radhanakrishnamurthy et al<sup>42</sup> have studied bulk magnetic properties including susceptibility studies at various temperatures on synthetic members of titanomagnetic series as a function of titanium content.

A polycrystalline material may contain :

- i) Multidomain (MD)
- ii) Single Domain (SD)
- iii) Super paramagnetic (SP) particles depending upon its thermal history. Any one of them can be made to predominate by the method of preparation. A.C. susceptibility and magnetisation explore existence of these particles, in the material. Hence we have carried out a susceptibility studies on our Co-Zn ferrite samples undoped and doped with Al and  $\text{Gd}^{3+}$ .

#### 4.13(a) SUSCEPTIBILITY :

The schematic curves of normalized a.c. susceptibility versus temperature for respective domain states viz. MD, SP, SD-UA, SD-CA are shown in Fig. 4.4

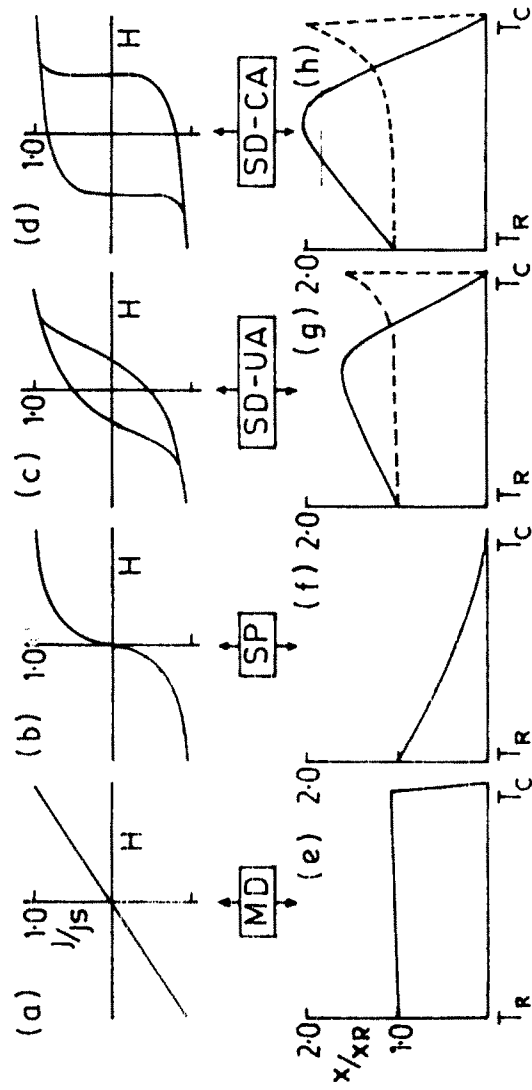


Fig 4.4 - Schematic hysteresis loops and normalised susceptibility versus temperature curves for samples consisting of different domain states:MD, multidomain:SP, superparamagnetic:SD-UA, single domain with uniaxial anisotropy:SD-CA, single domain with cubic anisotropy.

FOR M.D. PARTICLE :

The  $\chi_{ac} \rightarrow T$  or plot of  $\chi / \chi_{RT} \rightarrow T$  is invariant and drop suddenly near critical temperature  $T_c$ .

FOR S.D.PARTICLES :

The plot of  $\chi_{ac} \rightarrow T$  or  $\chi / \chi_{RT} \rightarrow T$  is characterised by broad hump below  $T_c$  or a sharp cusp near  $T_c$  depending upon blocking temperatur  $T_b$  at which SD become SP. The temperature at which cusp appears is called as freezing temperature and is associated with cooperative freezing of magnetic moments in random direction. The bump for (SD-CA) particle is intense than that for (SD-UA)

FOR S.P. PARTICLES :

The plots of  $\chi_{ac} \rightarrow T$  and  $\chi / \chi_{RT} \rightarrow T$  drops suddenly from room temperatue to zero at critical temperatur.

#### 4.13(b) HYSTERESIS AND DOMAIN STRUCTURE :

Bean has shown that three distinct loops can be obtained for different domain structure shown in (Fig. 4.4)

- 1 Large multidomain (MD)
- 2 Small interacting superparamagnetic (SP)
- 3 Optimum single domain particles with uniaxial anisotropy (SD-UA)

#### 4.14 EXPERIMENTAL MEASUREMENT OF $\chi_{ac}^T$ :

The variation of a.c. susceptibility with temperature was studied at Tata Institute of Fundamental Research (TIFR). The variation was recorded on "The susceptibility and Hysteresis Apparatus Model RMSH-III" which is very versatile and highly sensitive instrument for measurement of magnetic susceptibility of all kinds of specimen in an alternating magnetic field

##### PRINCIPLE :

A specimen kept in the centre of a balanced double coil which itself is at centre of a Helmholtz coil system producing an alternating magnetic field, behaves like an alternating dipole and induces differential e.m.f. in double coil. The current is supplied to Helmholtz coil by an oscillator and high quality power amplifier.

The signal induced in double coil is proportional to the rate of change of magnetic moment of specimen. The signal is then amplified, rectified and read out on a true r.m.s. digital voltameter (Model HIL 2615). The meter reading is calibrated in terms of magnetic moment. Knowing the magnetic field and volume of specimen, the susceptibility can be calculated. The sample in the form of finely ground sintered powder was enclosed in a glass jacket, in which thermocouple was placed to sense the temperature. The thermocouple used was plat-plat Iridium for all the samples. The field current

of 45 mA was adjusted and kept constant for all samples. The Helmholtz coil is provided with water circulation in order to maintain the temperature. The meter readings were recorded from room temperature  $25^{\circ}\text{C}$ . / <sup>Onward</sup> The glass jacket containing sample was removed slightly out of heating arrangement to record background effect and then was placed in contact with heating arrangement. Actual magnetic moment was calculated taking into consideration the background effect. The magnetic moments were observed at various temperatures starting from room temperature. The readings were taken, while heating as well as while cooling. It is observed in general that, as temperature increases susceptibility at first increases, reaches maximum and then goes on decreasing till it becomes zero. The temperature at which susceptibility become zero, is referred to as critical temperature of that specimen.

#### 4.15 RESULTS AND DISCUSSIONS :

In Fig. 4.5 variation of normalized susceptibility as a function of temperature has been given for the ferrite series  $\text{Co}_x \text{Zn}_{1-x} \text{Fe}_2\text{O}_4$  where  $X= 0.0, 0.3, 0.5, 0.7, 1.0$ . The following observations can be made :

1. The variation in susceptibility appears to be sensitively dependent on the concentration of cobalt in the system. The samples  $\text{CoFe}_2\text{O}_4$  (A<sub>5</sub>) and  $\text{Co}_{0.7}\text{Zn}_{0.3}\text{Fe}_2\text{O}_4$  (A<sub>4</sub>) show almost identical variation of normalised susceptibility as a function of temperature. In both these samples initially ( $T < 100^{\circ}\text{C}$ ) the

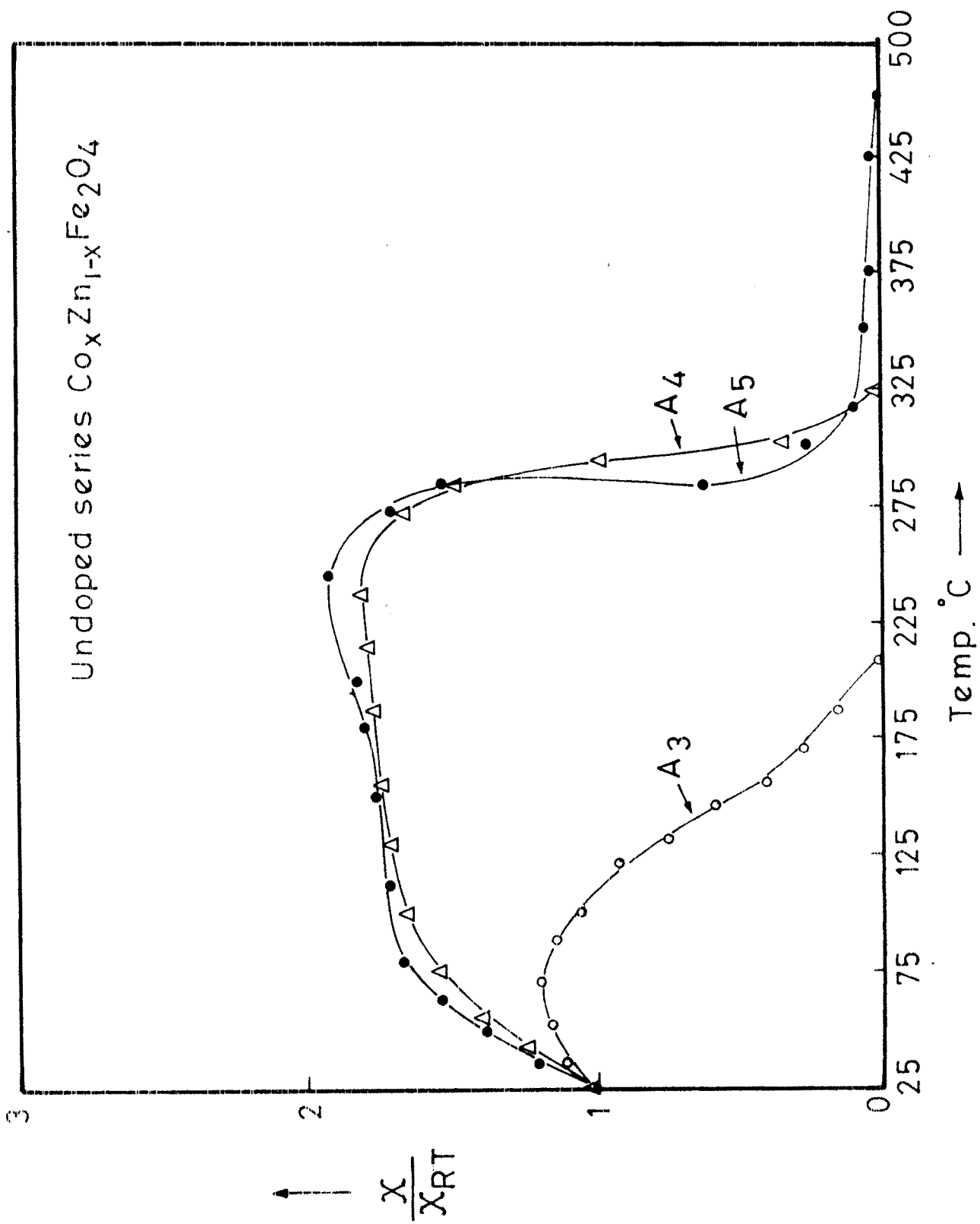


Fig.4.5

normalised susceptibility tends to increase with the increase of temperature. In the range  $100^{\circ}\text{C}$  to  $275^{\circ}\text{C}$  the susceptibility is invariant, whereas it drops sharply to zero near the Curie temperature for both the samples the sharp fall in susceptibility indicates that impurity phases are not formed within the samples. This fact is also confirmed from X-ray analysis.

2. For  $\text{Co}_{0.5}\text{Zn}_{0.5}\text{Fe}_2\text{O}_4$  the susceptibility initially tends to increase whereas after  $75^{\circ}\text{C}$ , the susceptibility gradually decreases. This shows that some impurity phases may be present in the material. In the XRD of the same samples. Two extra lines are observed indicating some other phases. The ferrite  $\text{Co}_x\text{Zn}_{1-x}\text{Fe}_2\text{O}_4$  with  $X = 0.1$  and  $0.3$  show non magnetic behaviour .

In Fig. 4.6 temperature variation of normalised susceptibility is shown for the series  $\text{Co}_x\text{Zn}_{1-x}\text{Fe}_2\text{O}_4$  doped with 0.05 At wt.% Al ( where  $X = 0, 0.3, 0.5, 0.7$  and  $1.0$ ) It is seen that the sample  $\text{Co}_{0.5}\text{Zn}_{0.5}\text{Fe}_2\text{O}_4$  (B<sub>3</sub>),  $\text{Co}_{0.7}\text{Zn}_{0.3}\text{Fe}_2\text{O}_4$  (B<sub>4</sub>) show identical behaviour i.e. as the temperature increases,  $\chi / \chi_{\text{RT}}$  remains temperature independent, whereas near the Curie point there is sharp fall in  $\chi / \chi_{\text{RT}}$ . The behaviour of sample B<sub>5</sub> however appears to be drastically modulated in comparison with A<sub>5</sub>. The susceptibility increases rapidly reaches the maximum value 8.5 between 700 to  $750^{\circ}\text{K}$ , while near Curie it drops very sharply.

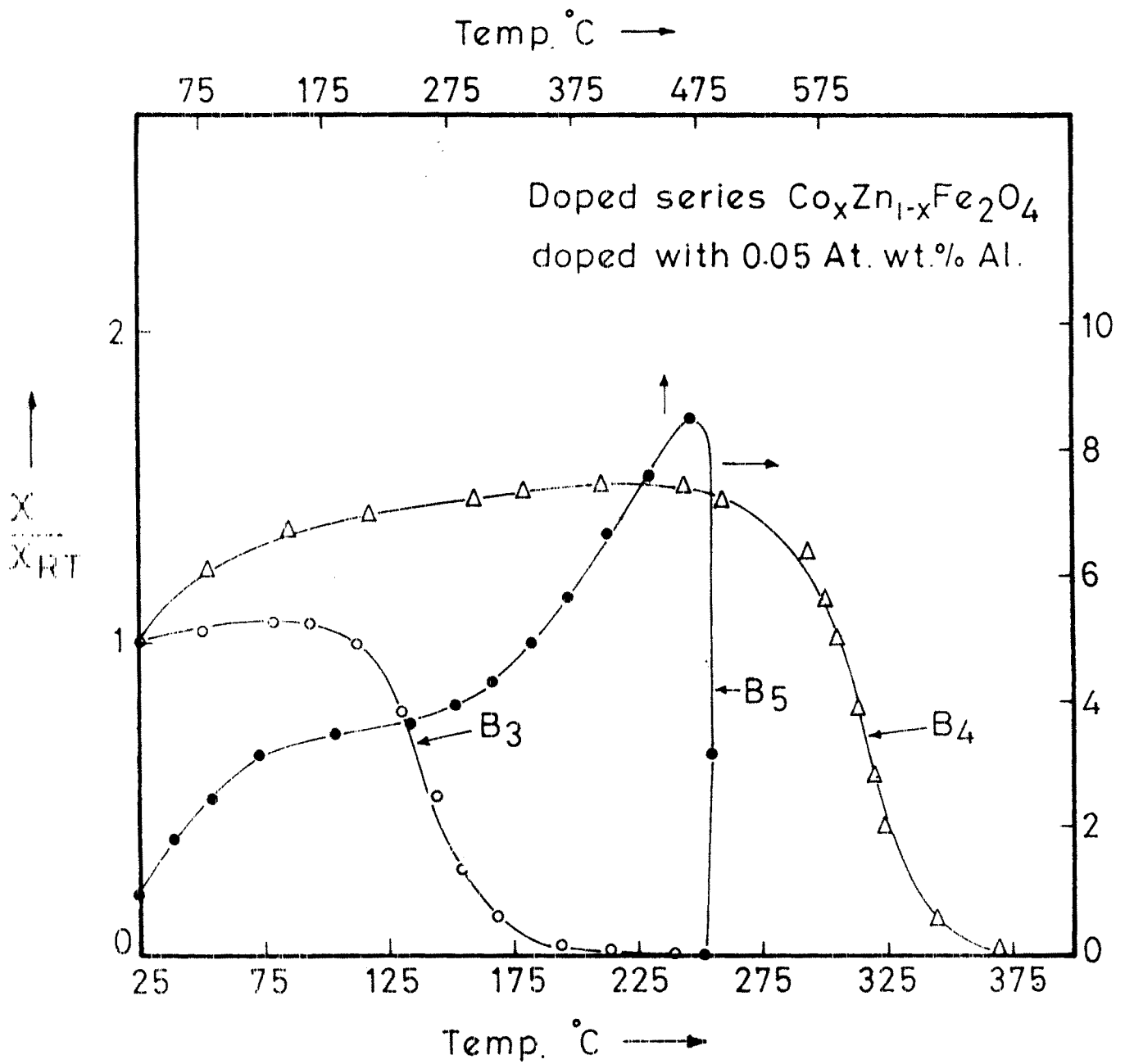


Fig. 4.6



In Fig. 4.7 variation of  $\chi/\chi_{RT}$  as a function of temperature has been given for ferrite series  $\text{Co}_x\text{Zn}_{1-x}\text{Fe}_2\text{O}_4$  (where  $x=0.0, 0.3, 0.5, 0.7$  and  $1.0$ ) doped with  $0.05$  mol wt. %  $\text{Gd}_2\text{O}_3$ . The following observations have been made :

1. In sample  $C_5$ ,  $\chi/\chi_{RT}$  increases as temperature is increased and near  $T_c$  there is sharp fall in  $\chi/\chi_{RT}$
2. In sample  $C_4$   $\chi/\chi_{RT}$  initially increases with temperature upto  $t = 100^\circ\text{C}$ , while for  $T > 100^\circ\text{C}$ ,  $\chi/\chi_{RT}$  remain constant and drop sharply near  $T_c$
3. In the sample  $C_3$ ,  $\chi/\chi_{RT}$  is temperature invariant and it drops gradually near  $T_c$ . Indicating the impurity may be present within this sample.

The demagnetised state of a ferro or ferrimagnetic substance is generally presumed to be due to its subdivision into Weiss Domains with Bloch Walls between them<sup>43</sup>. Grains which have domain walls in them are known as multidomain (MD).

Theoretical estimate of typical wall thickness is in the range of few hundred to few angstroms for different materials. Magnetic grains which are few hundred angstroms or even larger, and if particles are acicular cannot contain domain walls due to energy considerations and these are formed as a single Domain (SD) for which magnetisation direction is fixed in space. However, if the temperature of on SD is

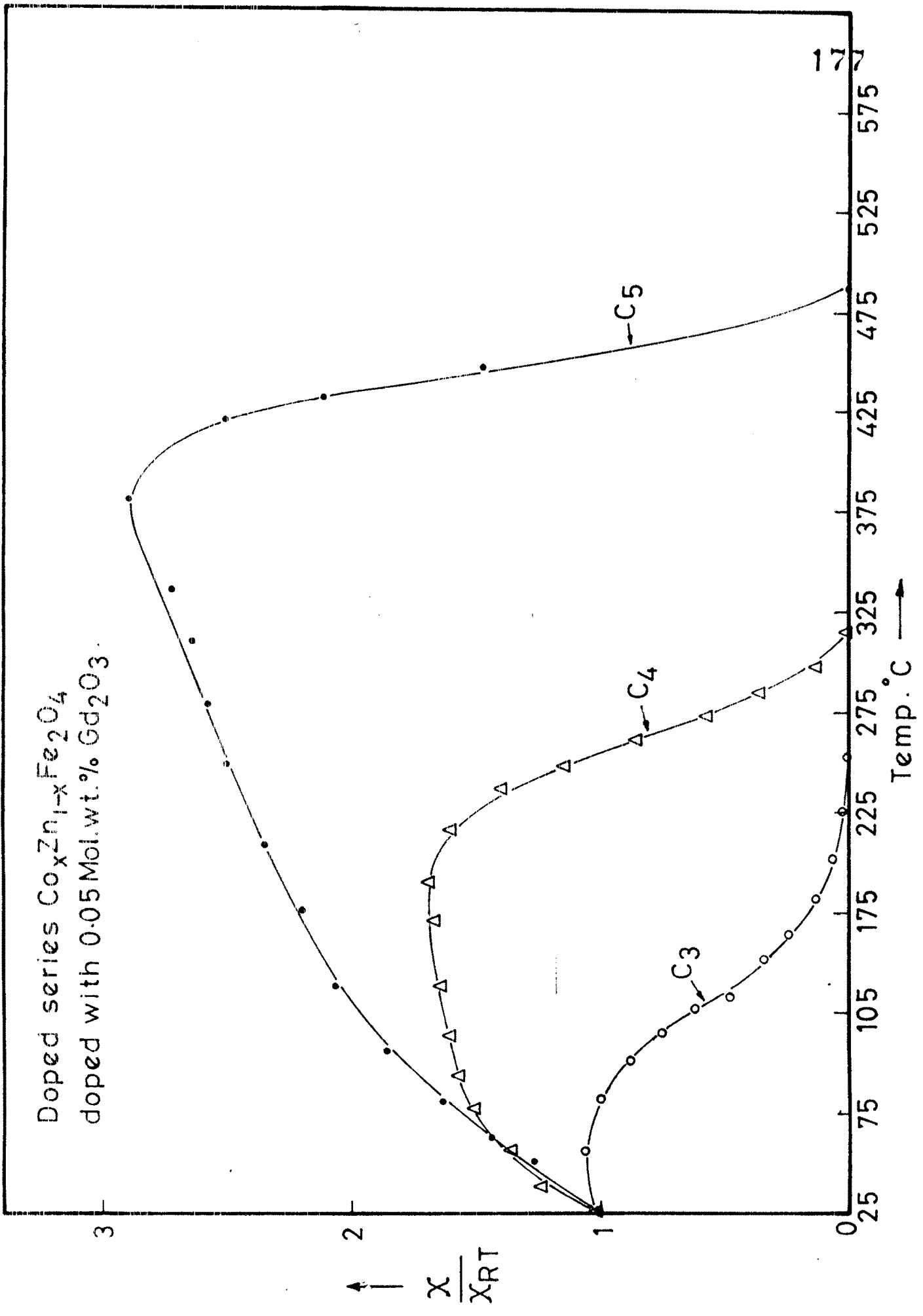


Fig. 4.7

increased it may so happen that the thermal energy may become comparable to the effective anisotropy energy, when the magnetisation direction fluctuates between the easy axis of grain. In such a state the grain is said to be exhibiting superparamagnetic (SP) and for the volume  $v$  of the grain, the temperature is referred to as the blocking temperature  $T_b$  which will be less than the Curie point  $T_c$  of the concerned material. These parameters are related as,

$$v J_s H_c = 2kT_b \quad 44$$

where  $J_s$  is saturation intensity

$H_c$  is coercive field

$k$  is Boltzmann constant

Hence the magnetic states of SD and SP are interchangeable by temperature. Although (SD) would be magnetised below  $T_c$ , a sample containing large number of them could have a net zero magnetisation due to a random orientation of their moments. Thus a polycrystalline material may consist of three types of states (MD, SD and SP) though any one of them may be made to predominant by an appropriate method of sample preparation and heat treatment.

Usually it is assumed<sup>45</sup> that, sample containing MD or SP particles of any material do not show any hysteresis however, practically some little hysteresis may arise due

to defects and stresses in (MD) samples and interaction effect in (SP) samples. By measuring the hysteresis parameters of the sample at low temperature, it is possible to deduce if it contains (SP) or (MD) for in the case of (SP) sample  $H_C$  and  $J_R$  tend to reach the values pertinent to (SD) case as temperature is lowered<sup>46</sup>, while for the (MD) case there would be only some marginal increase in the values of these parameters.

Thermal variation of initial susceptibility :

Magnetisation measurements, in low fields ( $\ll 10$  oe) and at high temperatures was first carried out on iron by Hopkinson.<sup>47</sup> He showed that it reaches a peak value just before  $T_C$  and becomes zero rapidly. For this type of measurement the sample is taken in the form of ring or long rod to avoid demagnetisation effects. However, many modern magnetic materials are made and used in the form of small lumps, pellets or micropowders. If such samples are used in low field magnetisation, the sharp fall below  $T_C$  could still be observed in case of MD samples, though the peak may be reduced considerably due to demagnetisation effects. The measured signals would be proportional to the apparent susceptibility  $\chi$ , which is related to real susceptibility  $\chi'$  by the relation<sup>4</sup>

$$\chi = \frac{\chi'}{1 + N\chi'}$$

when  $N$  is demagnetisation factor of the instrument. There would be three types of susceptibility peaks in  $\chi$ - $T$  curves.

- 1 Hopkinson peak is the one occurring just before the  $T_c$  of any magnetic material in (MD) state.
- 2 SD peak which could be obtained only if the sample under investigation has substantial proportion of SD particles in it and occurs at the  $T_b$  of the particles.
- 3 Isotropic peak which could be seen clearly for a magnetic material in MD form and only if the material has the temperature at which magnetocrystalline anisotropy is zero.

In contrast to low field measurement the use of high magnetic field obliterates the difference in magnetisation temperature ( $J_s-T$ ) curves of SD or MD samples, of any material. For pure ferromagnets the single Brillouin curve is obtained and ferrimagnets would show a resultant of two or more Brillouin curves.<sup>48</sup> It has been reported<sup>49</sup> that apparent magnetisation at 300K in the field of 9.2 KOe was zero for particles of size  $100 \text{ \AA}^0$   $\text{Mn}_{0.6}\text{Zn}_{0.4}\text{Fe}_2\text{O}_4$  and  $150 \text{ \AA}^0$  for  $\text{MnFe}_2\text{O}_4$ . Using this experimental fact and the equation ( $\gamma J_s H_c = 2kT_b$ ) it can be calculated that manganese ferrite particles of  $190 \text{ \AA}^0$  would show a zero apparent magnetisation in similar fields at 600 K, which is far from its  $T_c$  of 665 K. From these considerations, it could be expected that magnetic samples containing distribution of fine particles could show tails in  $J_s-T$  curves causing ambiguities in determination of  $T_c$ . A theoretical treatment of this aspect was given by Evdokimov.<sup>50</sup>

In the following discussion the series A is undoped samples and series B and C are of doped samples doped with Al and  $Gd_2O_3$  respectively. The suffix 1,2,3,4,5 indicates zinc content viz. 1 correspond to Zn content 1, 2 correspond to Zn content 0.7, 3 correspond to Zn content 0.5, 4 correspond to zinc content 0.3, 5 corresponds to Zn content 0. in  $Co_x Zn_{1-x} Fe_2O_4$

On observing susceptibility curves Fig. 4.5 . . , 4.6 4.7 for the samples  $A_3$ ,  $A_4$ ,  $A_5$  and  $C_4$ ,  $C_5$ . it can be stated that these samples contain SD particles, whereas the curves for  $B_3$ ,  $B_4$ ,  $C_3$  samples indicate presence of MD particles.

It is seen that doping affects  $\chi/\chi_{RT}$  characteristically at blocking temperature  $T_b$  increasing its value. Similarly comparing curves for sample ( $A_3, B_3, C_3$ ), ( $A_4, B_4, C_4$ ), it is noted that blocking temperature increases for  $Gd^{3+}$  doped samples, whereas it is reduced for  $Al^{3+}$  doped samples. This may be regarded as aluminium doping suppresses the magnetic properties, whereas Gadolinium doping enhances the same. This is supported by our magnetisation measurements. Also it is seen that the blocking temperature for these low in comparison with that for the samples  $A_5$ . This may be due to sufficient amount of zinc content in these samples, which favours SD to MD transition as indicated by slow fall of  $\chi/\chi_{RT}$  from the blocking temperature.

- 1) Addition of Aluminium in Co-Zn mixed ferrite system favours (SD + MD) particles.
2. Addition of  $Gd_2O_3$  tends to enhance  $T_b$  and retains SD behaviour.
- 3) Addition of zinc brings about SD to MD transformation. This is to be expected as pure zinc ferrite is nonmagnetic material.

## SECTION : C : CURIE TEMPERATURE :

## 4.16 INTRODUCTION :

The dependence of Curie temperature on the distribution of metallic ions on tetrahedral and octahedral sites in ferrite was suggested a long time ago by Gorter<sup>51</sup> and Neel<sup>52</sup>. Rezelescu et al<sup>53</sup> investigated the influence of preparation techniques and cation distribution on various properties of copper and manganese mixed ferrites. In zinc mixed ferrites, the A-B interaction decreases with increasing zinc ions and Curie point drops with the result of substitution of zinc. Forestier<sup>54</sup> studied the variation of Curie temperature of  $\text{Me}_x\text{Zn}_{1-x}\text{Fe}_2\text{O}_4$  [Me=Ni] with zinc content. Gorter<sup>51</sup> studied the Curie temperature of Barrium ferrite and suggested that the existence of a strong competing interaction in Barium ferrite causes a linear curve to occur for full occupation of magnetic ions of all sublattices.

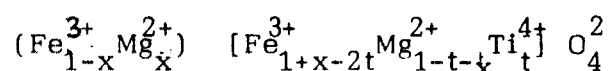
Study of tetravalent  $\text{Ge}^{4+}$ ,  $\text{Ti}^{4+}$  &  $\text{Sn}^{4+}$  ions substituted magnesium ferrite has been carried out by Sagar et al<sup>55</sup>. They found that Curie temperature decreases with the addition of tetravalent ions in simple magnesium ferrite. Similar behaviour in Curie temperature variation is reported by A.R.Das et al<sup>56</sup> in case of Ni-Zn ferrite, the substitution ions are  $\text{Ti}^{4+}$ ,  $\text{Zr}^{4+}$  and  $\text{Sn}^{4+}$ . However, on small  $\text{Ti}^{4+}$  substitution, the Curie temperature drastically falls and afterwards increases. Recently Semary et al<sup>57</sup> have reported that addition of  $\text{Ti}^{4+}$  in simple



Mg ferrite reduce the Curie temperature. They have suggested a variation between Curie temperature and content of Ti(t) and the concentration of Mg (x) as

$$(1+x) (1+x-2t) = (1-x^2) - 2t(1-x)$$

The following cation distribution has been suggested.



we have measured Curie temperature experimentally. The results are correlated with existing theory.

#### 4.17 CURIE TEMPERATURE DETERMINATION :

Curie temperature of the samples were measured from the expt. described below. Our experimental arrangement is an improved version of Loria's<sup>35</sup> expt. Fig.4.8

An electromagnet was kept above vertical furnace. Induction method is employed to magnetise the specimen bar to which pellet was attached. Curie temperature is measured using chromel Allumel thermocouple along with digital multimeter of least count 0.1 mV enabling measurement of temperature with accuracy of less than 5%. (PLATE III)

#### 4.18 RESULTS AND DISCUSSION :

In Fig. 4.9 variation of Curie temperature with content of zinc is shown for series A, B and C.

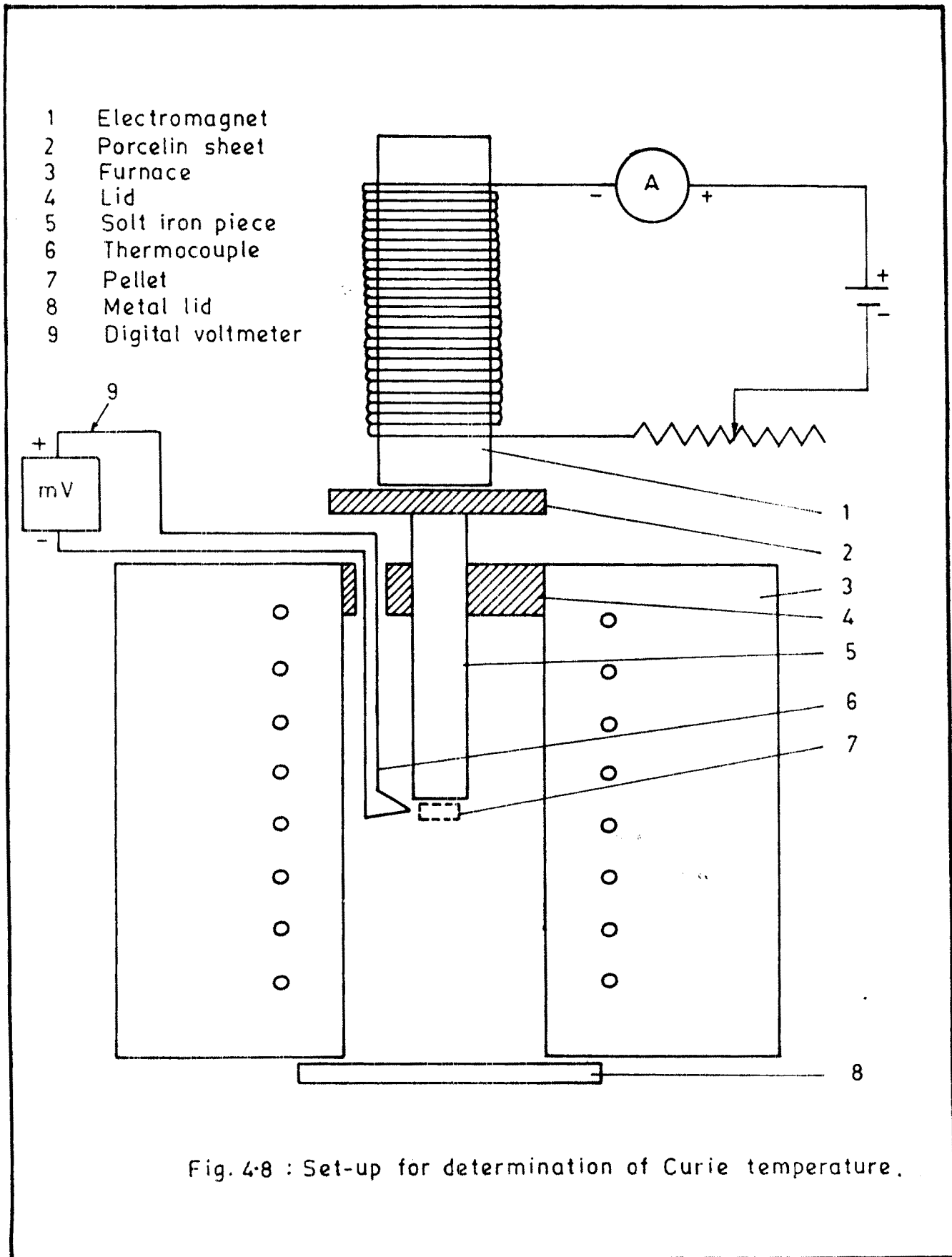


Fig. 4-8 : Set-up for determination of Curie temperature.

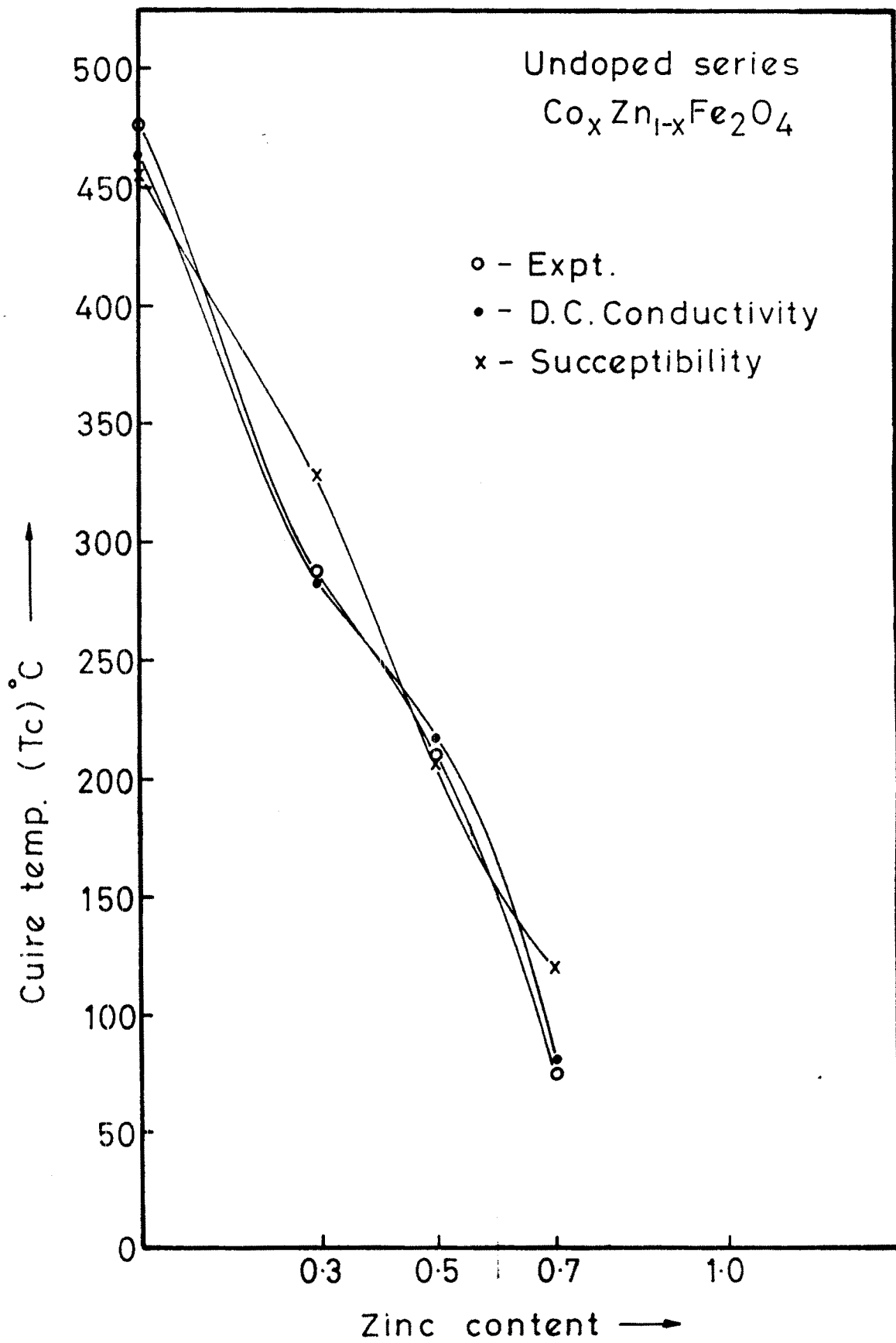


Fig. 4.9

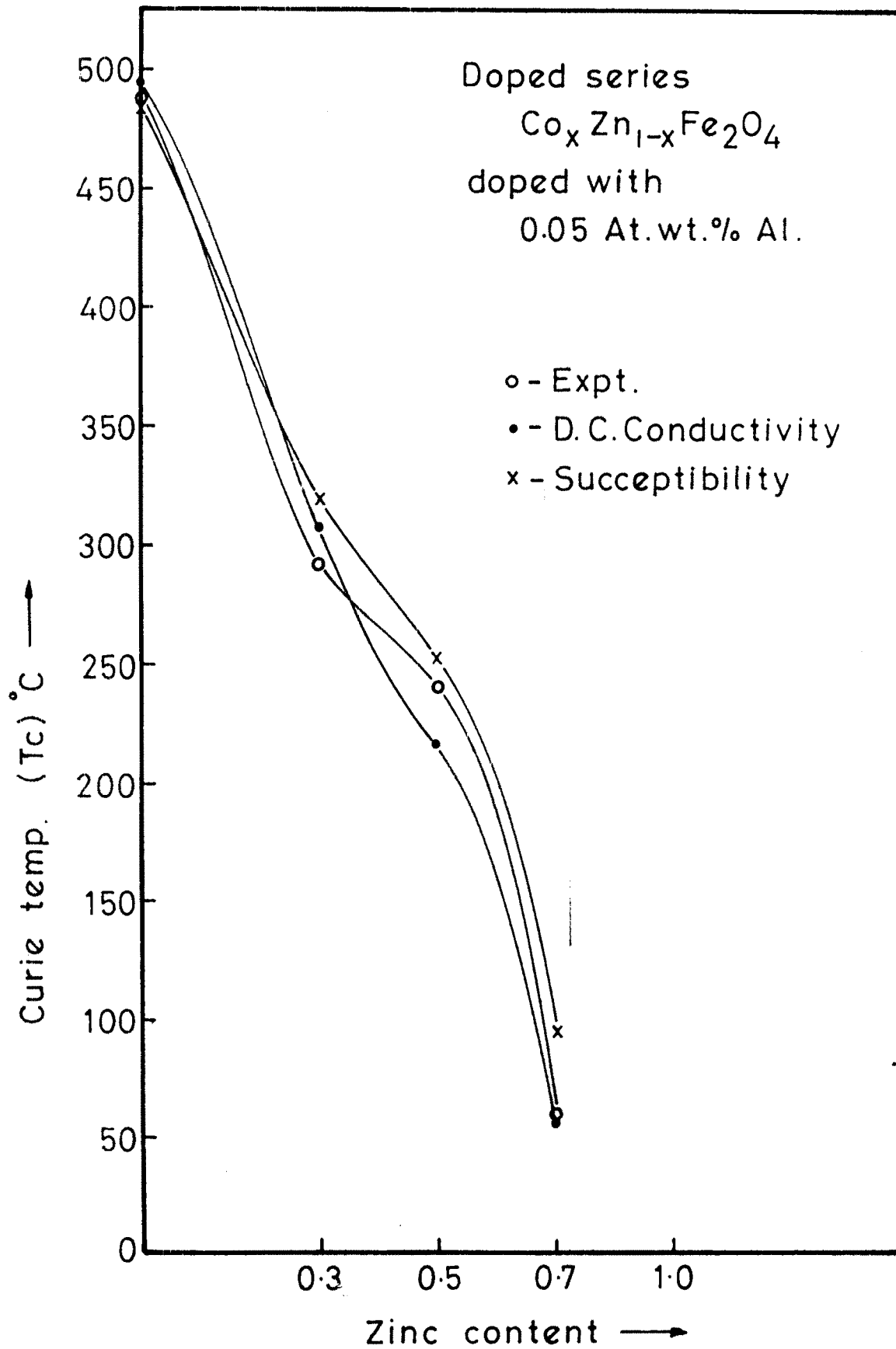


Fig. 4.10

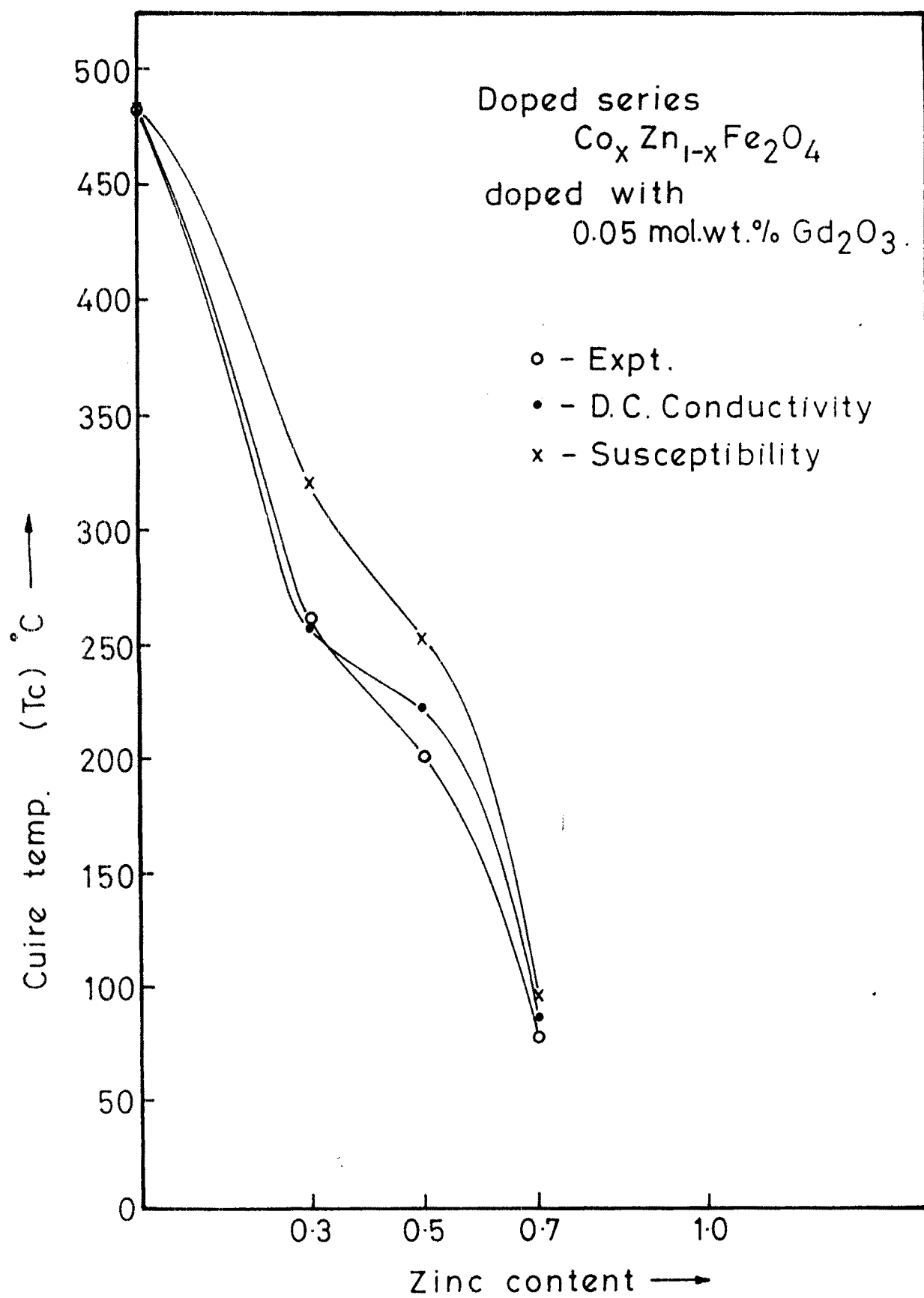


Fig. 4.11

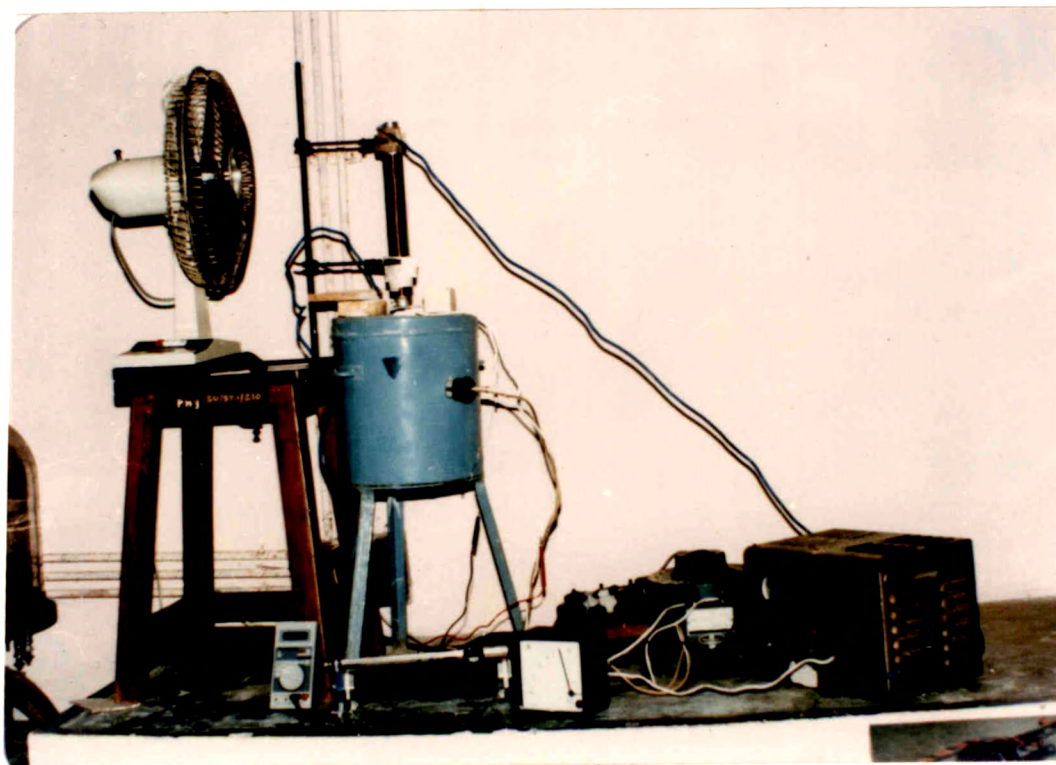


PLATE - III

TABLE 4.2  
CURIE TEMPERATURE

Series	Composition	Curie Temperature C <sup>o</sup>		
		From Experiment	From D.C. conductivity	Fro A.C. Susceptibility
A	Co <sub>0.3</sub> Zn <sub>0.7</sub> Fe <sub>2</sub> O <sub>4</sub>	75	<del>99</del> 73	119
	Co <sub>0.5</sub> Zn <sub>0.5</sub> Fe <sub>2</sub> O <sub>4</sub>	210	217	207
	Co <sub>0.7</sub> Zn <sub>0.3</sub> Fe <sub>2</sub> O <sub>4</sub>	287.5	282	327
	Co <sub>1.0</sub> Zn <sub>0.0</sub> Fe <sub>2</sub> O <sub>4</sub>	475	462	455
B	Co <sub>0.3</sub> Zn <sub>0.7</sub> Fe <sub>2</sub> O <sub>4</sub>	60	58	100
	Co <sub>0.5</sub> Zn <sub>0.5</sub> Fe <sub>2</sub> O <sub>4</sub>	240	218	239
	Co <sub>0.7</sub> Zn <sub>0.3</sub> Fe <sub>2</sub> O <sub>4</sub>	293	308	374
	Co <sub>1.0</sub> Zn <sub>0.0</sub> Fe <sub>2</sub> O <sub>4</sub>	487.5	496	495
C	Co <sub>0.3</sub> Zn <sub>0.7</sub> Fe <sub>2</sub> O <sub>4</sub>	80	84	94
	Co <sub>0.5</sub> Zn <sub>0.5</sub> Fe <sub>2</sub> O <sub>4</sub>	200	222	252
	Co <sub>0.7</sub> Zn <sub>0.3</sub> Fe <sub>2</sub> O <sub>4</sub>	260	270	319
	Co <sub>1.0</sub> Zn <sub>0.0</sub> Fe <sub>2</sub> O <sub>4</sub>	480	496	483

NOTE : Series A undoped Co<sub>x</sub>Zn<sub>1-x</sub> ferrite system

Series B doped series Co<sub>x</sub>Zn<sub>1-x</sub>Fe<sub>2</sub>O<sub>4</sub> doped with  
0.05 At.At.% Al.

Series C doped series Co<sub>x</sub>Zn<sub>1-x</sub>Fe<sub>2</sub>O<sub>4</sub> doped with  
0.05 mol. wt.% Gd<sub>2</sub>O<sub>3</sub>

it is seen that there is non linear decrease in the value of  $T_c$  on addition of zinc similar trend is observed by earlier workers. The nonlinear variation indicates that triangular type of spin arrangement is favoured. Similar trend is observed when the system is doped either with Aluminium (Al) and  $Gd_2O_3$  (Fig.4.10 and 4.11) respectively.

According to Neels model the magnetic interaction between  $Fe^{3+}$  ions and  $Fe^{3+} - Co^{2+}$  ions on A and B sites respectively via oxygen, govern the Curie temperature. Also the angle  $Fe_A^{3+} - O - Fe_B^{3+}$  and distances  $Fe_A - O$ ,  $Fe_B - O$  determine Curie temperature.

Zinc ion selectively occupy A site. On addition of zinc, zinc ions forces  $Fe^{3+}$  ions towards B site. In this way according to Neels theory there is a decrease in the product of  $Fe^{3+}$ ,  $Fe^{3+} - Co^{2+}$  ions, causing Curie temperature to decrease.

From Table 4.2 it is seen that as zinc content increases Curie temperature drops no matter whether samples are doped or undoped. It appears that  $T_c$  values are not significantly affected either by doping of Al or  $Gd_2O_3$ , so it can be concluded that doping does not markedly affect A-B interaction.



## R E F E R E N C E S

1. Neel L.  
Ann. Physique, J. 137 (1948).
2. Maxwell S.P.  
The marconi Rev. 1st Quarter (1970).
3. Weiss S.P.  
J. Physique 6, 661 (1901)
4. Heisenberg W.  
Zeit fur Phys 49, 619 (1928).
5. Neel  
Ann Physique J. 137 (1947).
6. Gorter E.W.  
Nature 165(798) (1950).
7. Gorter E.W.  
Phil Res. 9, 1 (1950)
8. Gorter E.W.  
Sci. Paris 230 192 (1950)
9. Gorter E.W.  
Phil Res 9, 321 (1954).
10. Pauthert R. and Bauchinrt L.  
J. Phys. Rad. 12, 249 (1951).
11. Pauthert R.  
Ann. Phys. Paris 7, 710 (1952).
12. Smit J. and Wing H.P.J.  
Ferites Philips Tech. Lab. (1959).

13. Verwey E.J.W. Romeijn F.C.  
J. Chem. Phys. 15, 181 (1947).
14. Verwey E.J.W., Doer F.D., Van Santen J.H.  
J.Chem.Phys. 16, 1091 (1948).
15. Bertaut E.F.  
J.Phys. Rad. 12 252 (1951).
16. Gillet M.J.  
J.Phys. Chem. Soli 13, 1877 (1960).
17. I.Shikawa V.J.  
Phys. Soc. Japan 17, 1877 (1962).
18. Krishnamurthy K.R.  
Ph.D. Thesis I.I.T. Madras (India) (1975).
19. Vologin V.G., Parkhomenko V.D. Dubinin S.F. Chaukarikin  
Yu.G. Goschitskij B.N. Siderao S.K. and Petrov V.V.  
Phys. State Col. (a) 33 K 83, (1976).
20. Appandairajan N.K.  
Ph.D. Thesis I.I.T. Madras (1980).
21. Sawant S.R. and Patil R.N.  
Solid State comm. Vol. 40, 391 (1981).
22. Sankpal A.M. Sawant S.R. Vaingankar A.S.  
Indian J.Phys. 62A 396, (1988).
23. Fallois and Marconi P.  
J.Phys. Rad 12, 256 (1951).
24. Guillaud C. and Creveaux  
compt. Rend. 230, 375

25. Nowik L.  
J.Appl. Phys. 40, 812 (1969).
26. Nowik L.  
J.Appl. Phys. 40, 5184 (1969).
27. Resenewaig A.  
Can J.Phys. 48, 2857 (1950).
28. Guillaud and Creveaux C.R.  
Acad Sci. Paris 230 1256 (1950).
29. Yafet Y. and Kittel C.  
Phys.Rev. 87 290 (1967).
30. Zener C.  
Phys. Rev.96, 1335 (1954).
31. Barkhausen H.  
Phys. Zeit 20, 401 (1919).
32. Heisenberg W.  
Zeit Fur Phys. 74, 295 (1932).
33. Bloch F.  
Zeit Fur. Physics 74, 295 (1932).
34. Kersten M.  
Hirzel Leipzig (1943) Grundlagen Ciner Theorieder  
Ferromagnetischen Hysterese under Kuerzitivkraft
35. Guillaud C.  
Properties Magnetic der ferrite J.De phys.Radium  
(1951) 912-21.

35. Loria K.K. and A.P.B. Sinha  
Ind.J.Pure and Appl. Phys Rev. B-19 499 (1979).
36. Sawant S.R. and Patil R.N.  
J. App.Vol. 21, PP 145. (1983).
37. Baldha G.J. and Upadhyay R.V.  
Mater Res. Bull Vol. 21 1051, (1986).
38. Kulkarni R.G. and Upadhyay R.V.  
Mater Res. Bull Vol. 4, No.3 168 (1986).
39. Chaugule R.J. and C.Radhanakrishnamurthy Sampatkumaran  
E.V., Mulik S.K., Vijay Raghavan R.  
Mat. Res. Bull. Vol. 18 817 (1983).
40. Neel L.  
Compt Rend 228 664 (1949).
41. S.R.Sawant, D.S. Birajdar, S.S. Suryavanshi, A.M.Sankpal  
B.L.Patil, R.N.Patil  
Indian Journal of Pure and Appl. Phys Vol. 28  
July (1990) PP 424-426.
42. C.Radhakrishnamurthy and S.D.Likhite E.R. Deutch  
G.S.Murthy.  
Phys. of Earth and Planetary Interiors, 30(1982)PP 281-90
43. Radhakrishnamurthy C and Nandikar N.G.  
Pramana Vol.13. No.4. 413, (1979) .
- 44/ Neel L.  
Adv. Phy.4 , 191, (1955).

45. Bean C.P.  
Journal APP. Phys. Vol. 26, 1381, (1955).
46. Berkowitz A.E and Scheuele W.J.  
J. Appl. Phys. 30, 1345, (1959).
47. Hopkinson  
J. Phil Trans. R.Soc. (London) A-180, (1889).
48. Smit J. and Wijn H.P.J.  
Ferrites Philips Tech. Library P.30. (1959).
49. Sato T, Kuroda C, Saito M.  
Proc. International Conf. Japan University, Park  
Press P-72, (1970).
50. Eydokimov V.B.  
Russ. J.Phys. Chem. 38, 1080, (1964).
51. Gorter E.W.  
Phil Re.s Rept. 9, 321 (1954).
52. Neel L.  
Ann. Dec. Phy. 3, 137, (1948).
53. Rezelescu N., Istrate S., Rezelescu E., Lucu E.J.  
Phys. Cehm. Solidi 35, 43 (1974).
54. Forester H.
55. Sagar D.R. Chandra Prakash Chatterjee S.N. Pran Kishan  
Proc. of International Conf. on ferrites. ICF-5  
441 (1989).
56. Das A.R.
57. Semary M.A., Ahmed M.A. Abbas, Y.  
J. Mat. Sci. 18, 2890 (1983).